Laser-Induced Spark Ignition of CH_4/Air Mixtures

TRAN X. PHUOC* and FREDRICK P. WHITE

Federal Energy Technology Center, U.S. Department of Energy, P.O. Box 10940, MS 84-340, Pittsburgh, PA 15236-0940, USA

Laser-induced spark ignition of CH_4-air mixtures was experimentally investigated using a nanosecond pulse at 1064 nm from a Q-switched Nd-Yag laser. Laser irradiance in the order of 10^{12} to 10^{13} W/cm^2 was found to be sufficient to ignite a mixture having from 6.5 to 17% methane by volume (equivalence ratio, ER, from 0.66 to 1.95). The dependence of the breakdown threshold laser energy, E_{thr}, on the gas pressure was in agreement with the electron cascade theory. Depending on the laser energy, E_o, the spark absorption coefficient in the range from 0.1 to about 100 cm^{-1} was calculated using the electron-ion inverse bremsstrahlung process. The minimum ignition energy was about one order of magnitude higher than the minimum ignition energy obtained by the electric spark ignition. It had its lowest value remaining at about 3 to 4 mJ for a mixture having 10 to 15% methane by volume (ER = 1.058 to 1.68) and it increased sharply toward the far-lean and the far-rich sides of the stoichiometry. The average length and radius of the spark for a stoichiometric or near-stoichiometric methane–air mixture were about 0.8 mm and 0.3 mm, respectively. For lean or rich methane–air mixtures, the average long axis of the spark size varied from about 0.8 to 2 mm, whereas for the short axis it varied from about 0.4 to 1.2 mm depending on the methane volume fraction.

NOMENCLATURE

c	velocity of light
d	beam diameter
E	laser pulse energy
E_{max}	maximum laser energy
E_o	time-averaged laser energy
E_{thr}	breakdown threshold laser energy
e	electronic charge
F_{ph}	photon flux
F_E	electric field
f	focal length
g_i	Gaunt factor
h	Planck's constant
K_v	absorption coefficient
k	Boltzmann's constant
l	focal point spot length
m_e	electron mass
n_e	number of electron density
n_i	number density of the ith ionic species
P_w	laser power
p	pressure
r	focal point spot radius
r_{shck}	shock radius
t	time
T	temperature
z_i	charge of the ith ionic species

Greek

γ	c_p/c_v, specific heat ratio
θ	beam divergence
λ	laser wavelength
v	shock velocity
v_o	sonic velocity
ρ_o	density
τ	laser pulse duration
τ_{FWHM}	full width at half maximum (FWHM) pulse duration
τ_o	calculated by Eq. 2

INTRODUCTION

Interest in laser ignition has increased in recent years because of its many potential benefits over conventional ignition systems. Many potential applications and benefits were reviewed by Ronney [1]. In general, laser ignition is nonintrusive and is capable of providing multiple ignition sites that can be programmed to ignite a combustible mixture either sequentially or simultaneously. Problems such as wall effects, heat loss through the electrodes, partial burn, and misfire can be avoided. In addition, if a flame is initiated simultaneously at many points throughout the mixture volume, the total burning time could be much smaller. This could be potentially important for fuel-lean combustion applications.

*Corresponding author. E-mail: tran@fetc.doe.gov

There are generally three mechanisms by which laser radiation can ignite a combustible solid, liquid, or gaseous mixture: laser-induced thermal ignition, laser-induced photochemical ignition, and laser-induced spark ignition.

In the laser-induced thermal ignition, laser radiation is used to heat and increase the target temperature. As a result, molecular bonds are broken and chemical reactions take place. This type of ignition has been successfully applied for gaseous mixtures, such as H_2/O_2, CH_4/O_2, CH_3OH/O_2, and C_2H_5OH/O_2, [2–7]. Hill and Laguna [5] and Hill [6] studied the effects of the laser duration on the ignition of $SF_6/CH_4/O_2$ mixtures at pressures from 75 torr to 200 torr using a pulsed TEA CO_2 laser. They reported that ignition by the 0.25-μs pulse laser requires 20% less absorbed energy than ignition by the 0.82-μs pulse. This is because a greater part of the laser energy is concentrated in the SF_6 molecules during the shorter duration pulse, resulting in an initially large concentration of highly excited SF_6 and F atoms. The contribution of these species to the ignition is such that less absorbed energy is required for ignition with the short duration pulse than with the long duration pulse. Trott [7] studied the CO_2-laser-induced deflagration of many fuel/oxygen mixtures with laser intensities <5 J/cm^2, duration of 100 ns, and test gas pressures from 85 to 100 torr. These conditions were carefully selected so that effects due to infrared laser photochemistry could be avoided. The author reported that the importance of the complex energy absorption, the hydrodynamic motion, and acoustic instabilities generated by thermal expansion during the induction period should be accounted for in order to quantitatively interpret the ignition results.

This ignition mechanism can easily be used to ignite solids because of the absorption ability of the solids at infrared wavelengths. However, it is subject to some important limitations when it is used to ignite gaseous systems. First, a combustible mixture with strong absorption at the laser wavelength must be used. In some cases, gases such as SF_6, SiF_4, NH_3, and CH_3F are used as inert, resonant absorbers at CO_2 laser wavelength, but none of these compounds has proved entirely satisfactory. Second, complications associated with nonthermal components, such as photodissociation, hydrodynamic motion, and acoustic instabilities, might complicate the ignition process.

Laser-induced photochemical ignition can include resonant breakdown and resonant photochemical ignition. In resonant breakdown, a target molecule is dissociated by a nonresonant multiphoton dissociation process. The atom produced is then ionized by a resonant multiphoton ionization process. The electrons produced this way absorb more photons, leading to the formation of microplasmas. Forch and Miziolek used this technique to ignite H_2/O_2 and H_2/N_2O mixtures near 225.6 nm, and premixed gaseous flow mixtures of H_2/O_2 and D_2/O_2 near 243 nm [8–10].

In resonant photochemical ignition, laser photons dissociate the target molecules into highly reactive radical species. If the rate of production of these radicals is greater than their recombination rate, they will initiate the usual chemical chain-branching reactions leading to ignition and full-scale combustion [11–16]. Norrish [11] obtained ignition and combustion of C_2H_2/O_2, CH_4/O_2, and C_2H_4/O_2 mixtures due to the developing chains initiated by the OH radical. Lavid and Stevens [13] and Lavid et al. [14] studied the photoignition of unsensitized premixed H_2/O_2 and H_2/air mixtures using laser radiation at 157, 193, and 245 nm wavelengths. In their studies, the dissociation of molecular oxygen was responsible for ignition. Chou and Zukowski [15] investigated the ignition of H_2/O_2, H_2/air, and CH_4/O_2 mixtures in an open air-flow system at 1 atm and room temperature using excimer laser radiation operated at 193 nm. NH_3 was added as a photosensitizer. They concluded that the ignition of these mixtures was due to chain-branching reactions initially involving H and NH_2 radicals produced from photolysis of NH_3.

Because the photochemical ignition process requires laser energy typically in the order of less than a millijoule [11, 13–15], it does not involve photoionization or direct heating [12]. In fact, the technique can be used to ignite a combustible mixture if a sufficient amount of reactive radicals (in the order of 10^{17} atoms/cm^3 [12–15]) within a sufficiently large volume is produced. Thus, the crucial factors that determine whether or not ignition occurs are the

concentration of radicals produced by photon absorption, and the volume in which the radicals are contained—not the laser energy density. This might be a major difference from thermal ignition where a minimum ignition energy and a minimum size are required.

When thermal energy is deposited into an ignition volume, part of this energy is lost and part of it is used to heat the surrounding gas, leading to ignition. Such a thermal ignition process can be characterized by a long chemical induction time (milliseconds) and a short excitation time (microseconds). The induction time is the time from the initial heating to the onset of rapid temperature rise. During the induction period, reactive radicals required to sustain chain-branching reactions are built up, and during the excitation period, strong exothermic reactions occur leading to steady combustion reactions. If radicals, instead of thermal energy, are initially deposited, the heat loss and radical build-up processes are avoided. For this reason, it is expected that photochemical ignition has shorter ignition time, and it can be used to ignite a combustible mixture under conditions that are normally unignitable.

However, there are many disadvantages to the use of photochemical ignition for practical applications. First, a particular laser or a laser that is tunable might be required to provide the wavelength that matches with the target molecule's absorption wavelength in order for dissociation to occur. Second, since the photon energy at visible and near-IR wavelengths is smaller than the dissociation energy of most gases, the photochemical ignition process is most effective at UV wavelengths. At present, such lasers are expensive, and compact, lightweight lasers for practical combustion applications are not yet available.

In laser-induced spark ignition, laser irradiance in the order of 10^{10} W/cm^2 (or laser photon flux in the order of 10^{29} photons/cm^2-s) is sufficient to generate a spark plasma at the end of the laser pulse, either by the multiphoton ionization process or the electron cascade process. In the multiphoton ionization process, a gas molecule absorbs a sufficient number of photons. If the photon energy absorbed is higher than its ionization potential, the gas molecule is ionized. This process is important only at very short wavelengths (<1 μm) or at very low pressures (<10 torr), where collisional effects are negligible. It becomes insignificant at visible and near-IR wavelengths because the photon energy at these wavelengths is much smaller than the ionization potentials of most gases. For example, the photon energy for a CO_2 laser is 0.1 eV, and for an Nd-Yag laser at 1.064 μm it is 1.0 eV, while the ionization potentials for most gases are larger than 7 eV. Thus, the multiphoton ionization process would require the absorption of 70 CO_2 photons (or 7 Nd-Yag photons) to ionize most gases. This is highly difficult.

The electron cascade requires the existence of initial electrons. The electrons then absorb more photons via the inverse bremsstrahlung process. If the electrons gain sufficient energy, they ionize other gas molecules on impact, leading to an electron cascade and breakdown of the gas. At high pressure ($\geq$100 torr) and long wavelength (≥ 1 μm) this process usually dominates the gas breakdown. For ignition application, the creation of a laser spark is usually associated with this process.

The initial electrons from which an electron cascade can develop can be generated by the multiphoton ionization process, if the laser irradiance is high enough. To provide the required irradiance, laser beams are typically pulsed at a Q-switch pulse duration of nanoseconds, and focused into a small volume (in the order of μm). The presence of impurities, such as aerosol particles or low ionization-potential organic vapors, can also significantly facilitate the generation of the initial electrons.

A spark produced in this way has time scales much shorter than the kinetic time scale and the chemical induction time. It is apparently a localized point source of highly reactive chemical intermediates. Its temperature (in the order 10^6 K) and pressure (in the order of 10^3 atm) can be reached at the end of the laser pulse. This extreme condition relative to the ambient gas leads to the development of a rapidly expanding shock wave that is of sufficient strength to ignite a gaseous combustible mixture [17–22], liquid fuel sprays [23, 24], or even to extinguish a diffusion flame [18].

Lee and Knystautas [17] used a Q-switched ruby laser with 10 ns duration pulse to investi-

gate the laser-spark ignition of stoichiometric propane–air mixtures and equimolar acetylene–oxygen mixtures with and without nitrogen dilution. They reported that the effects of chemical reactions during the initial stage of the blast wave expansion are negligible, and the ignition mechanism strongly couples with the dynamics of the decaying blast. As the blast expands, the reaction front decouples rapidly from the shock and propagates as a deflagration wave dependent on the transport properties of the medium. Schmieder [18] used multipulses of a CO_2 TEA laser of 1 μs duration to produce cylindrical sparks 2 to 3 mm long, and 0.5 mm in diameter to ignite and extinguish a methane jet diffusion flame. The results showed that the same laser-induced spark could successfully extinguish the flame at much greater distances than those at which it ignited it.

Spiglanin et al. [19] studied laser-induced spark ignition of hydrogen/air mixtures. By observing the shape and structure of the developing flame kernels, they concluded that (1) early flame kernel growth is dominated by the gas motion induced by the short duration spark, and (2) the ultimate fate of an ignition depends on the chemistry of the reactions, which determines whether the gas could undergo a transition from hot plasma to propagating flame. These might be the factors that strongly influence the minimum ignition energy. The excessive values of the laser energy density required to create a spark can cause blast-wave losses and turbulent disturbances that can disrupt the natural evolution of the spherical flame. As a result, the spark kernel might require higher energy to undergo a transition to propagating flame.

Syage et al. [20] measured the ignition energy of H_2/air mixtures of different equivalence ratios using output at 1064, 532, and 355 nm of a Nd-Yag laser operating either as a Q-switched nanosecond laser or a pulse-mode-locked picosecond laser. They reported minimum ignition energies that are higher than the electric-discharge ignition energies and that increase toward the fuel-lean and rich side of the stoichiometry. A similar trend was also reported by Lim et al. [22] for methane–air mixtures. Ma et al. [21] conducted experiments on laser spark ignition of methane–air mixtures under pressures typically found in internal combustion (IC) engines. The experiment used a four-stroke, single-cylinder, high-pressure combustion chamber. Laser beams from an excimer laser (248 and 193 nm) and from a Nd-Yag laser (1064 nm) were used. They reported that the ignition time by laser spark is about 4 to 6 ms shorter than the ignition time by electric spark, and it is independent of the laser energy and wavelength. The results indicate that at a sufficiently high kernel energy density, addition of more energy does not contribute to ignition enhancement. An extra energy pulse, in fact, can add to plasma heat.

Laser-induced spark ignition is more favorable because it does not require a close match between the laser wavelength and the target molecule's absorption wavelength to create a spark [20]. Although laser wavelength influences the threshold for breakdown, once breakdown is achieved, ignition depends only on the amount of energy absorbed in the plasma. Thus, the laser irradiance at the focal volume, not the laser wavelength, is the only crucial requirement. This present work is designed to look into many fundamental issues, such as spark formation, ignition energy, spark size, spark absorption, and developments associated with the laser-induced spark ignition of methane–air mixtures.

EXPERIMENTAL APPARATUS

A sketch of the experimental apparatus is shown in Fig. 1. The apparatus had a cylindrical shape and was made out of stainless steel with an inside diameter of 62.5 mm, and a length of 37.5 mm. To allow viewing of the entire volume of the chamber, the chamber ends were fitted with windows (75 mm diameter) of either quartz glass or fused silica. The cell had several ports around its periphery. Two ports were equipped with an entrance, and exit windows. The other ports were used for gas inlets, gas outlet, and for mounting a pressure sensor. This configuration allowed for a variety of selectable environments, and for monitoring the pressure inside the cell. As a safeguard, the cell was connected to a 5-liter safety buffer cylinder via a solenoid valve. The solenoid valve was controlled by an elec-

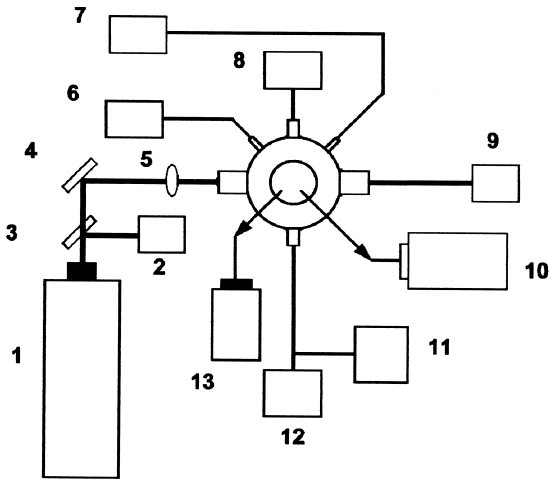

Fig. 1. Sketch of the experimental apparatus: (1) Nd-Yag laser; (2) and (9) pyroelectric energy detectors; (3) 10% beam splitter; (4) mirror; (5) 7.5 mm focal length lens; (6) and (7) gas inlets; (8) pressure transducer; (10) PMT unit; (11) and (12) safety cylinder and vent; and (13) imaging unit.

tronic control circuit that was activated by the digital signal fed from the pressure sensor. A successful ignition generated a large pressure rise, and the solenoid valve was activated to evacuate the ignition cell when the pressure rise reached 2000 torr.

Laser energy at 1064 nm wavelength was generated by a single-mode, Q-switched Nd-Yag laser (Quantel, Brilliant W). The laser beam was delivered and focused into the ignition cell using a 75 mm-focal length lens. The lens was mounted on a translational stage so that the focal point inside the chamber could be moved. Pulse duration of 5.5 ns and pulse energies up to 200 mJ were used for the present experiments. The laser energy delivered to the ignition cell was controlled by the laser potential controller and a laser attenuator (Molectron JA-YAG-50).

Several diagnostic devices were used to study the laser-induced ignition process. A high-speed digital video system was used to record spark formation and growth. Time-resolved pressure measurements were made at the wall of the ignition cell, approximately 3.15 mm from the ignition spark using a piezoelectric pressure transducer. Two pyroelectric energy meters (LaserProbe RJP734) were used for spark energy measurements. One meter was placed behind the exit window facing the incoming laser beam, and the other was placed after a 10% beam splitter which was located before the entrance window. A LaserProbe ratiometer (LaserProbe RJ7620) was used to compare the energy levels detected by the two meters. This arrangement allowed the energy meters to detect the transmitted beam through the ignition cell with and without breakdown.

Time-resolved emission spectra of the OH radical in the ignition process were recorded using a 12-nm bandwidth interference filter centered at 308 nm and a PMT/Spectrometer combination unit. The spectrometer was apertured to view the entire volume of the cell. Ignition was easily distinguished from other processes giving rise to light emission by substantial rises in pressure and temperature in the combustion cell, coupled with the obvious luminosity and duration of the flame.

Methane (Matheson, research grade with 99.99% purity), and air from high pressure cylinders were delivered to the ignition cell using a gas handling system with precise gas flow controllers. In order to have a good combustible mixture with accurate fuel-to-air proportions the cell was first evacuated. Fuel was then injected into the cell using a needle valve, and the fuel pressure inside the ignition cell was monitored. Next, air was injected and allowed to circulate inside the cell in a turbulent pattern. The composition of fuel and air was determined by the pressure of each gas. The mixture inside the cell was then left to stabilize for 5 to 10 minutes before testing.

RESULTS AND DISCUSSIONS

For a Q-switched pulse of a laser operating in a single longitudinal mode, the pulse energy of a temporal pulse shape that is Gaussian in time is given as

$$E(\tau) = E_{max} \exp(-\tau^2/\tau_o^2), \quad (1)$$

where E is the pulse energy (J), E_{max} is the maximum laser energy, τ is the time, and τ_o is the time at which $E(\tau_o) = E_{max}/e$, ($e = 2.7183$). Let τ_{FWHM} be the pulse duration (full width at half maximum) [FWHM]. Then τ_o is calculated from the following relation:

TABLE 1

Laser Energy and Power for the Present Experiments

Laser Energy, E_o (mJ)	Power, P_w (W)	Irradiance (W/cm^2)	Photon Flux, F_{ph} (Photons/cm^2-s)	Electric Field, F_E (V/cm)
15	2.56×10^6	1.14×10^{12}	6.08×10^{30}	2.17×10^7
200	3.41×10^7	1.52×10^{13}	8.10×10^{31}	7.97×10^7

$$\tau_o = \frac{\tau_{FWHM}}{2\sqrt{\ln 2}}; \tag{2}$$

the average laser energy, E_o, over τ_o is given as

$$E_o = \frac{1}{\tau_o}\int_{-\infty}^{\infty} E(\tau)\, d\tau$$

$$= \int_{-\infty}^{\infty} P_w \exp(-\tau^2/\tau_o^2)\, d\tau, \tag{3}$$

where P_w is the laser power (W); and P_w relates to E_o by the following:

$$P_w = \frac{E_o}{\tau_o\sqrt{\pi}}. \tag{4}$$

If the focal region of the beam is assumed to be cylindrical in shape, the spot size, in terms of radius, r, and length, l, is given as

$$r = \left(\frac{2\lambda}{\pi}\right)\left(\frac{f}{d}\right) \tag{5}$$

and

$$l = (\sqrt{\pi} - 1)\,\frac{\theta}{d} f^2, \tag{6}$$

and the electric field, F_E (in V/cm), and the photon flux, F_{ph} (in photon/cm^2-s,) are

$$F_E = \left(\frac{4P_w}{r^2 c}\right)^{1/2} = 11.55\left(\frac{P_w^{1/2}}{r}\right) \tag{7}$$

and

$$F_{ph} = \frac{P_w\lambda}{\pi r^2 hc} = 1.7 \times 10^{18}\left(\frac{P_w}{r^2}\right), \tag{8}$$

where f is the focal length, λ is the laser wavelength, d is the beam diameter, θ is the beam divergence (mrad), and c is the velocity of light. For the present study, $\lambda = 1.064$ μm, $f =$ 7.5 cm, $\theta = 0.5$ mrad, and $d = 0.6$ cm. With a pulse duration (FWHM) of 5.5 nanoseconds, $r = 8.46$ μm, $l = 194$ μm, and $\tau_o = 3.3$ ns. For E_o of 15 and 200 mJ, as used in this work, the calculated laser power, photon flux, irradiance, and electric field are tabulated in Table 1.

Numerous tests were conducted and showed that mixtures having less than 6.5% or more than 17% methane by volume (equivalence ratio [ER] = 0.61 to 1.95) were not ignitable even with laser energy, E_o, up to 200 mJ. E_o of less than 35 mJ did not ignite any mixture. In this case, only a slight increase in the pressure was observed at the wall. For mixtures having 6.5 to 17% methane, ignition was successfully obtained for all tests with E_o higher than 35 mJ. A successful ignition was detected based on three distinct pieces of information: the time-resolved pressure measurement, the time-resolved emission spectra of the luminous OH radical, and the rapid water condensation, which was seen on the observation windows. Figure 2 shows a typical chart of the cell pressure during an ignition event. The chart clearly

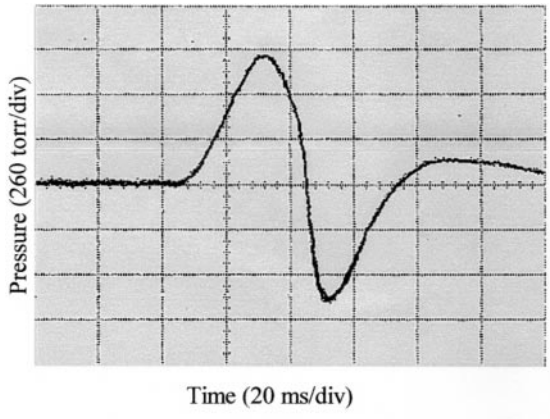

Fig. 2. Typical time-resolved pressure chart of an ignition event (stoichiometric methane/air at 1 atm, $E_o = 49$ mJ).

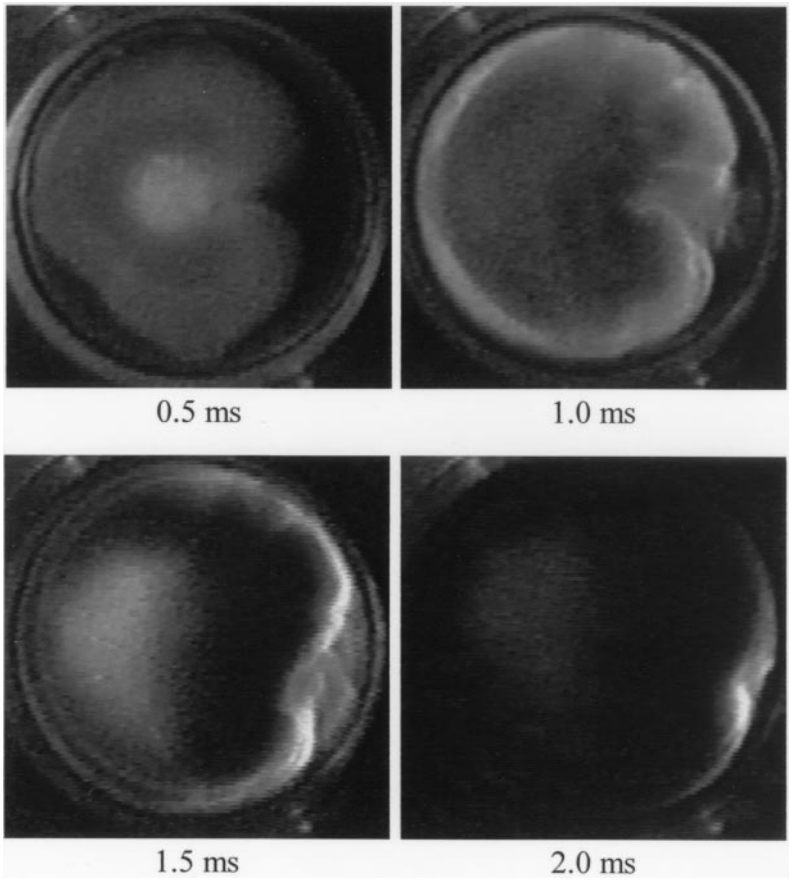

Fig. 3. Images of the laser spark ignition of a stoichiometric methane/air mixture at 1 atm and ignition spark energy of 5 mJ.

shows a rapid pressure rise, indicating that the mixture was ignited, followed by a rapid pressure drop, which was due to the water condensation on the cell wall and optics. Images of the ignition process (Fig. 3) indicate that the intense spark was created immediately after the laser pulse was fired. A loud cracking noise due to breakdown was always heard with the spark formation. The spark grew and was followed by a burst of a blue flame enveloping the spark. The flame then propagated rapidly to the cell wall where water vapor condensed.

Figure 4 shows a comparison of measured and calculated breakdown threshold laser energies, E_{thr}, versus pressure for air and methane. The breakdown was easily determined because it was always associated with a cracking noise, the appearance of the bright flash of light in the focal region, and the abrupt absorption of the laser pulse transmitted through the focal region. Our experiments showed that when high laser energy was used, gas breakdown occurred easily and it was reproducible. When the laser energy was reduced to its breakdown threshold value, gas breakdown became a sporadic event, and the threshold laser energy for initiating gas breakdown could vary by more than 50%. Such sporadic behavior might be due to the difficulty of generating the initial electrons at the breakdown threshold values. The breakdown threshold was then defined as the laser energy at which the gas would break down on more than 50% of the shots.

The results show that when the pressure was lower than 17 torr, gas breakdown was not possible for the range of laser energies used. When the gas pressure increased from 17 to 1010 torr, the threshold laser energy decreased drastically from 190 to 15 mJ. The sparks in the air were very bright, whereas those produced in

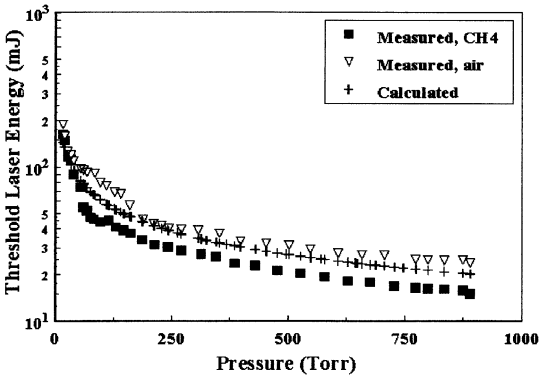

Fig. 4. Comparison of measured and calculated breakdown threshold laser energies versus pressure for air and methane. The calculations were done using $E_{thr} = \mathrm{K} \times \mathrm{P}^{-2/n}$ with $n = 4$ and $\mathrm{K} = 605$.

methane had a pinkish color. The breakdown threshold laser energies for air were slightly higher than the those for methane. Minck [25] showed that the electric field intensity required to produce a breakdown goes up exponentially as the initial pressure of the gas decreases. Armstrong et al. [26] and DeMichelis [27] reported that a threshold irradiance in the order of 2×10^{11} W/cm^2 (10^{29} photons/cm^2-s) is required to generate the initial electrons for electron cascade breakdown to develop at 1 atm. The results shown in Fig. 4 are in agreement with these studies.

The strong pressure dependence presented here for the threshold laser energies is clearly incompatible with the multiphoton ionization process, which predicts a very weak pressure ($p^{-1/2n}$) dependence for the threshold electric field [27]. To check if the present results could be described by the electron cascade theory, we compared our experimental results with the thresholds predicted by the electron cascade theory, represented by the following relation [28]:

$$E_{thr} \propto p^{-2/n}, \tag{9}$$

where p is the pressure. Using $n = 4$ (which is for gases with ionization potential of 7 eV, [27]) and a proportionality constant of 605, Eq. 9 yielded results which agreed very well with the measured thresholds. Thus, the present data on breakdown thresholds at various pressures are in agreement with the cascade theory.

The absorption coefficients of air and methane are shown in Fig. 5. By using the arrangement for the two pyroelectric energy meters

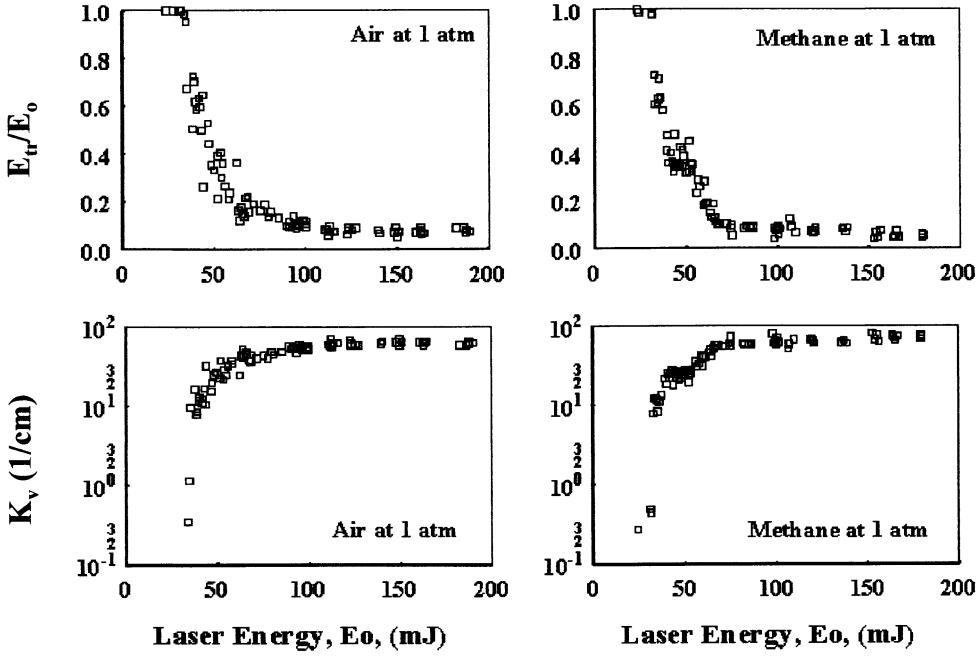

Fig. 5. Dependence of the laser energy transmitted through the focal volume, E_{tr}/E_o, and the absorption coefficients, $K_{v,air}$ and $K_{v,ch4}$ on the initial laser energy E_o.

described previously, the transmitted laser energies through the ignition cell, with and without breakdown, were measured in the following manner. First, the cell was evacuated to about 10 torr or less, the laser was fired, and the laser energy transmitted through the ignition cell was recorded. The cell was then filled with methane or air, and the laser was fired again. The spark energy was determined by comparing the energy transmitted through the cell in the presence of breakdown against that in the absence of breakdown. The attenuation of the laser energy in the presence of breakdown is attributed to spark absorption and the scatter of the laser light by the developing spark plasma. However, as discussed by Syage et al. [20] and Ma et al. [21], losses due to diffraction are negligible, and such an attenuation can be considered to be due solely to the absorption by the spark.

The absorption coefficients were calculated using the Beer-Lambert relation:

$$\frac{E_{tr}}{E_o} = \exp(-K_v l), \tag{10}$$

where E_{tr} is the laser energy transmitted through the focal volume of length l (cm) given by Eq. 6, and K_v is the absorption coefficient (1/cm).

It was obvious that when E_o was below its breakdown threshold level, air and methane were virtually transparent at the experimental laser wavelength, and the laser energy was transmitted through the focal volume without attenuation. When E_o reached its breakdown threshold, a spark was generated, and the laser energy was strongly attenuated. Depending on E_o, the absorption coefficients were in the range from 0.1 to about 100 cm^{-1} for both air and methane. Ma et al. [21] calculated the absorption coefficient for a methane–air mixture to be 22.8 cm^{-1} at 1.064 μm, which is in the range reported by the present study.

If it is assumed that the absorption of the laser energy by the spark is primarily due to the electron-ion inverse bremsstrahlung process, in which light is absorbed as a result of free–free transitions of the electrons in the field of the ions, then, with the information on K_v in Fig. 5, the kernel temperature can be estimated. It has been reported that when air is approximately 1% ionized, the effective absorption coefficient for inverse bremsstrahlung can be calculated using the following equation [29]:

$$K_v = \left[1 - \exp\left(-\frac{hc}{\lambda kT}\right)\right]\left(\frac{4e^6\lambda^3}{3hc^4 m_e}\right) \cdot \left(\frac{2\pi}{3m_e kT}\right)^{1/2} n_e \sum z_i^2 n_i g_i, \tag{11}$$

where n_e is the electron number density ($1/cm^3$), k is Boltzmann's constant (1.3803×10^{-16} erg/K), h is Planck's constant (6.6237×10^{-27} erg-s), c is the speed of light (2.9978×10^{10} cm/s), m_e is the electron mass (9.109×10^{-28} g), e is the electronic charge (4.8029×10^{-10} abs-esu), z_i is the charge of the ith ionic species, n_i is the number density of the ith ionic species ($1/cm^3$), and g_i is the Gaunt factor. For the study wavelength, Eq. 11 becomes

$$K_v = 0.1645 \times 10^{-34} \frac{n_e^2}{T^{1/2}\cdot} \cdot \left[1 \cdot - \exp\left(-\frac{13.5 \times 10^3}{T}\right)\right]. \tag{12}$$

To calculate the kernel temperature, the electron density must be known. Values of n_e in the order of 10^{19} cm^{-3} have been reported. Hauer and Baldis [30] estimated that, in spanning the range of laser irradiance from 10^{12} to 10^{16} W/cm^2, the background electron temperature varies from a few eV to several keV, and the critical electron density for a given laser wavelength is proportional to $10^{21}/\lambda^2$ (λ is in μm). Thus, for the present experimental wavelength, the critical electron density is in the order of 10^{20} cm^{-3}. Using the absorption coefficient presented in Fig. 5, the kernel temperature was calculated at about 8.8×10^5 to 1.4×10^6 K, which is in agreement with the reported kernel temperatures of about 10^5 to 10^6 K [19, 21, 27].

The minimum ignition energies of methane–air mixtures of different methane volume fractions were measured following the manner described above. It is clear from Fig. 6 that the minimum ignition energies remained at their lowest values of about 3 to 4 mJ for mixtures having about 10% methane (ER = 1.058) to 15% methane (ER = 1.68). They then increased sharply to about 40 mJ at 6.5% methane (ER =

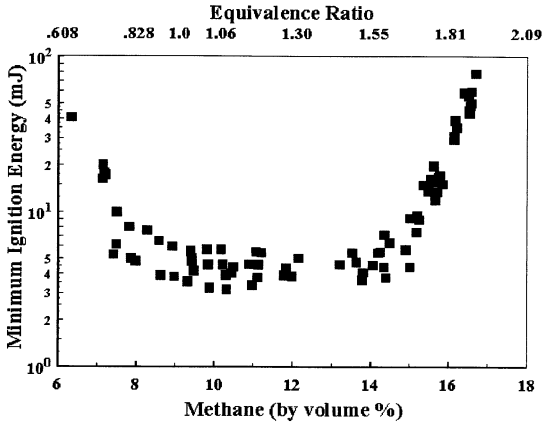

Fig. 6. Measured minimum ignition energies of methane/air mixture at 1 atm as a function of methane volume fraction.

0.66) and about 70 mJ at 17% methane (ER = 1.95). Increases in the minimum ignition energies toward both the lean side and the rich side of the stoichiometry are similar to the reports of Lim et al. [22] on the minimum laser ignition energies of CH_4/air mixtures and Syage et al. [20] on the minimum ignition energies of H_2/air mixtures. The minimum ignition energies reported here for stoichiometric methane–air mixtures at 1 atm are similar to those reported by Lim et al. [22] for a picosecond laser, but are higher than those measured by a nanosecond laser beam by a factor of about 3. The present result is also about one order of magnitude higher than the minimum ignition energy reported by Lewis and von Elbe [31] using electric spark ignition (about 0.4 mJ) and the computational prediction of Sloane [32] and Sloane and Ronney [33] using detailed chemical, hydrodynamic, and transport models (about 0.5 mJ for ER = 0.55, 0.10 mJ to 0.122 mJ for stoichiometric ratio, and 0.7 to 0.8 mJ for ER = 1.33). Syage et al. [20] reported the minimum ignition energies of stoichiometric hydrogen-air mixtures to be about 0.2 mJ, which is about 10 times higher than the minimum ignition energy reported by Lewis and von Elbe [31] using electric discharge (0.02 mJ).

Such a high minimum ignition energy can be attributed to several properties, such as short pulse duration and the small focal volume associated with the laser beam. For electric discharge ignition, the spark duration is long, the magnitude of the spark energy is small, and the disturbance of the flowfield by the decaying shock wave is negligible. The kernel expands in an almost quiescent gas, and the ignition mechanisms are diffusion-controlled. However, a spark created by focusing a picosecond or nanosecond laser pulse provides a different ignition mechanism. Such a spark can ignite a mixture directly, or by the force of the shock wave, or by the hot gas that remains after expansion. The rapid dissipation of energy and the small spark size increase the heat loss and limit the time that the energy will remain within the relevant dimension of the minimum flame kernel. The laser spark kernel will decay rapidly to the ambient condition without heating the surrounding gas to a temperature higher than the ignition temperature for a time longer than the chemical induction time. Thus, one must increase the energy source.

The rapid expansion and dissipation of energy of a laser-induced spark can be modeled as a Taylor blast-wave process, a model that has been used by many researchers to calculate the radius, velocity, temperature, and pressure of a laser-induced spark that required a high-power threshold to induce breakdown [18–20]. The relevant time-dependent equations of radius, temperature, pressure, and velocity of the spherical shock wave are expressed as [34, 35]

$$r_{shck} = (E_{sp}/\rho_o)^{1/5} t^{2/5}, \tag{13}$$

$$v = \frac{2}{5}(E_{sp}/\rho_o)^{1/2} r_{shck}^{-3/2}, \tag{14}$$

$$p = \left[\frac{2}{\gamma + 1}\right]\rho_o v^2, \tag{15}$$

and

$$T = T_o\left[\left(1 - \frac{v_o^2}{v^2}\right)\left(\frac{\gamma - 1}{\gamma + 1}\right) + 1\right] \cdot \left[\left(\frac{v^2}{v_o^2} - 1\right)\left(\frac{\gamma - 1}{\gamma + 1}\right) + 1\right], \tag{16}$$

where r_{shck} is the shock radius; v and v_o are the shock velocity and the sonic velocity, respectively; $\gamma = c_p/c_v$ is the specific heat ratio; p is the peak pressure; and T is the peak temperature.

Figure 7 shows these properties versus time for energy inputs of 0.4 and 10 mJ. For both

levels of the energy input, the initial temperature and pressure were in the order of 10^5 K and 10^3 atm, respectively. These conditions resulted in a strong shock wave that expanded into the combustible gas with significant high velocity. This shock wave then dispersed heat to the surrounding area, reducing the energy density within the kernel. The blast wave continued to move with significant velocity, and dissipates its energy over a dimension greater than the minimum ignition kernel volume. For 0.4 mJ energy input, the blast wave decayed rapidly to an ambient condition within 1 μs and at a radius of about 0.78 mm. For 10 mJ energy input, it continued to expand over a dimension and a time scale that were typically comparable to the minimum ignition kernel volume and induction time, respectively.

Ronney [1] discussed that, in addition to the minimum ignition energy, ignition also requires an optimum spark kernel radius to which the flame must grow after the spark energy is deposited. The need for an optimum spark size was also shown by the present work by comparing the laser energy required for ignition and the breakdown threshold laser energy for a given fuel–air mixture. It was observed that the minimum ignition energies remained the same for mixtures having methane from 8% to about 15%, and that, as the laser energy reached its breakdown threshold level, spark was created and ignition ensued. This indicates that the spark size at its breakdown threshold level is sufficiently large for ignition to develop. However, mixtures having methane too lean or too rich were not ignited by the spark that was created at breakdown threshold laser energy. This is because the sparks created are too small to be able to ignite a lean or rich mixture. Therefore, higher laser energy is required to create a larger spark to ignite these mixtures. For example, at 9.5% methane by volume (ER = 1.0) both spark and ignition occurred when laser intensity was at 39.2 mJ, while for a mixture of 7.2% methane by volume (ER = 0.74) a spark was formed at 32 mJ and ignition occurred at 39 mJ. For a mixture of 16% methane by volume (ER = 1.81) spark formation occurred at laser intensity of 60 mJ but ignition happened at 100 mJ.

Along with the minimum ignition energies

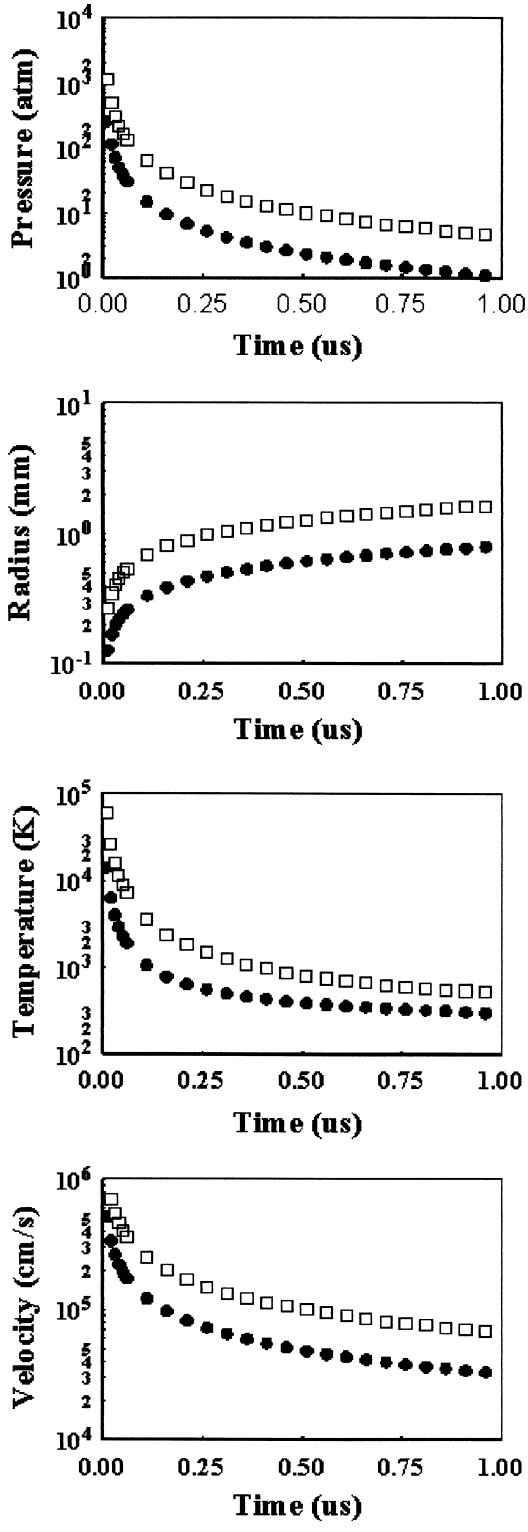

Fig. 7. Properties of an expanding laser-induced spark for stoichiometric mixture of methane and air at 1 atm. Input energies are 0.4 mJ (solid circles) and 10 mJ (open squares).

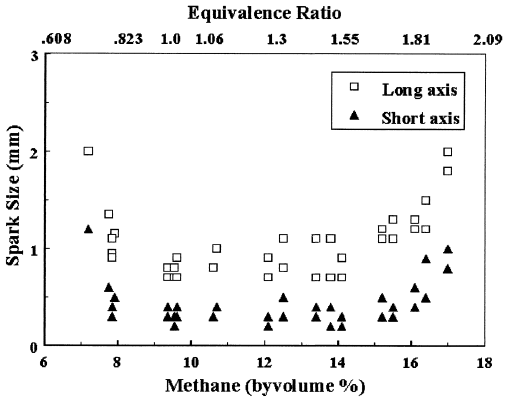

Fig. 8. Measured ignition spark sizes of methane/air mixtures at 1 atm versus methane volume fraction.

discussed above, we also measured the spark size required for ignition. In the present work, the spark sizes were measured using a slow-scan charge-coupled device (CCD) camera system. The camera was positioned to view the sparks in the direction perpendicular to the direction of the laser beam. A photomultiplier tube (PMT) was used with 1:1 imaging optics for time-resolved spark emission measurements. The spark size was then determined in terms of the FWHM of the emission intensity profile. The results are shown in Fig. 8, and images of the sparks are presented in Fig. 9. It was observed that the laser-induced spark was created after the laser was fired for about 270 to 350 ns. The spark had a short life (about 5 to 11 μs, depending on the laser energy) and was elongated in the direction of the laser beam. Separation of the spark plasma into several points along the laser beam and behind the focal point was also often observed (not shown in Fig. 9). For methane-lean or rich mixtures, the spark had an oval shape, its average long axis varied from about 0.8 to 2 mm, and its short axis varied from about 0.4 to 1.2 mm, depending on the methane volume fraction. For stoichiometric and near-stoichiometric methane–air mixtures, the spark became cylindrical in shape; its length and radius were about 0.8 mm and 0.3 mm, respectively. The results are in the same order with the minimum flame kernel radius of 0.3 mm reported by Lewis and von Elbe [31]. In comparison with other laser-induced spark studies, our results are very much in agreement with the results reported by Klimkin et al. [36], Spiglanin et al. [19], and Song and Alexander [37, 38]. In comparison with the report of Lim et al. [22], our results are similar to theirs for a nanosecond laser beam, but for the long axis for a

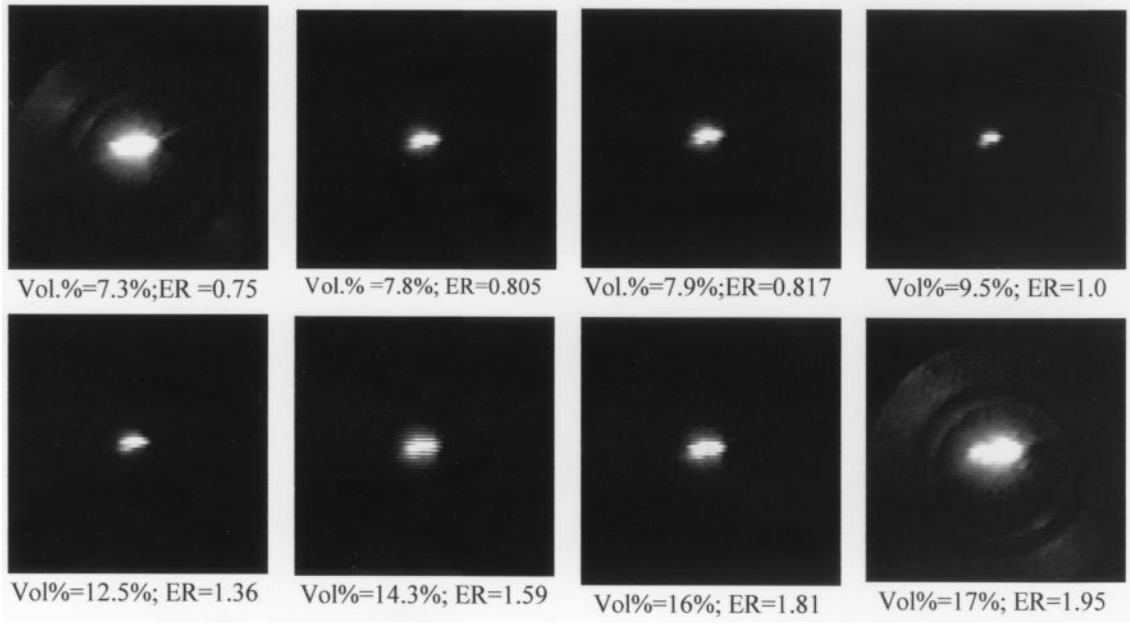

Fig. 9. Images of ignition spark size for CH_4–air mixture as a function of methane concentration by volume (or equivalence ratio, ER).

picosecond laser beam, our results are longer than theirs by a factor of 4.

CONCLUSIONS

Laser-induced spark ignition of methane–air mixtures has been experimentally investigated. Laser irradiance in the order of 10^{12} to 10^{13} W/cm^2 is sufficient to ignite a mixture having from 6.5 to 17% methane by volume (ER = 0.66 to 1.95).

The strong pressure dependence presented here for the threshold laser energy is clearly incompatible with the multiphoton ionization process, which predicts a weak pressure dependence for the threshold electric field. However, it agrees with the electron cascade theory. The spark absorption mechanism can be described by the electron-ion inverse bremsstrahlung process. For both air and methane, the absorption coefficient is in the range from 0.1 cm^{-1} to about 100 cm^{-1}, depending on the laser energy.

The results on the minimum ignition energy show an increase of the ignition energy toward the lean and the rich side of the stoichiometry. The minimum ignition energy is about one order of magnitude higher than the minimum ignition energy observed for the electric spark study. This notable trend might be due to the different ignition mechanisms between laser spark and electric spark ignition. It is noticed that, since the lower and upper limits of flammability of methane–air mixtures are 5% and 14 to 15% methane, respectively [31], a flame having a methane volume fraction within these limits could be sustained if it could be ignited, and a flame having a methane volume fraction outside these limits could not be sustained. Even an infinite amount of energy would not ignite such a flame. The present results, however, show that laser-induced spark ignition successfully ignites a mixture having a methane volume fraction up to 17%, which is richer than the upper limit of flammability, but it fails to ignite a mixture of less than 6.5% methane, which is higher than the lower flammability limit. Thus, laser-induced spark ignition works poorly at fuel-lean conditions, but it favors fuel-rich conditions. This is different from electric-spark ignition, which favors stoichiometric conditions.

The spark sizes and shapes reported here are found to be similar to those reported by other laser-ignition studies [19, 22, 36–38]. It is important to notice that although the spark sizes were measured at the minimum ignition energy, they might not necessarily be the minimum ignition spark sizes. In fact, the flatness of the minimum ignition energies (Fig. 6) and the minimum ignition spark sizes (Fig. 8) for mixtures having 8 to 15% methane suggests that the sizes might be larger than the minimum size required for ignition.

REFERENCES

1. Ronney, P. D., *Optical Engin*. 33:510 (1994).
2. Raffel, B., Warnat, J., and Wolfrum, J., *Appl. Phys*. B37:189 (1985).
3. Maas, U., Raffel, B., and Wolfrum, J., *Twenty-First Symposium (International) on Combustion*, The Combustion Institute, Pittsburgh, 1986, p. 1869.
4. Arnold, A., Hemberger, R., Herden, R., Ketterle, W., and Wolfrum, J, *Twenty-Third Symposium (International) on Combustion*, The Combustion Institute, Pittsburgh, 1990, p. 1783.
5. Hill, R. A., and Laguna, G. A., *Optics Communica*. 32:435 (1980).
6. Hill, R. A., *Appl. Optics* 20:2239 (1981).
7. Trott, W. M., *J. Appl. Phys*. 54:118 (1983).
8. Forch, B. E., and Miziolek, A. W., *Optics Lett*. 11:129 (1986).
9. Forch, B. E., and Miziolek, A. W., *Combust. Sci. Technol*. 52:151 (1987).
10. Forch, B. E., and Miziolek, A. W., *Combust. Flame* 85:254 (1991).
11. Norrish, R. G. W., *Tenth Symposium (International) on Combustion*, The Combustion Institute, Pittsburgh, 1965, p. 1.
12. Lucas, D., Dunn-Rankin, D., Hom, K., and Brown, N. J., *Combust. Flame* 69:171 (1987).
13. Lavid, M., and Stevens, J. G., *Combust. Flame* 60:195 (1985).
14. Lavid, M., Nachshon, Y., Gulati, S. K., and Stevens, J. G., *Combust. Sci. Technol*. 96:231 (1994).
15. Chou, M. S., and Zukowski, T. J., *Combust. Flame* 87:191 (1991).
16. He, L., and Clavin, P., *Twenty-Fifth Symposium (International) on Combustion*, The Combustion Institute, Pittsburgh, 1994, p. 45.
17. Lee, J. H., and Knystautas, R., *AIAA J*. 7:312 (1969).
18. Schmieder, R. W., *J. Appl. Phys*. 52:3000 (1981).
19. Spiglanin, T. A., Mcilroy, A., Fournier, E. W., and Cohen, R. B., *Combust. Flame* 102:310 (1995).
20. Syage, J. A., Fournier, E. W., Rianda, R., and Cohen, R. B., *J. Appl. Phys*. 64:1499 (1988).

21. Ma, J. X., Alexander, D. R., and Poulain, D. E., *Combust. Flame* 112:492 (1998).
22. Lim, E. H., McLLroy, A., Ronney, P. D., and Syage, J. A., in *Transport Phenomena in Combustion* (S. H. Chan, Ed.), Taylor & Francis, London, UK, 1996, p. 176.
23. Liou, L. C., *Laser Ignition in Liquid Rocket Engines*, 30th AIAA/SAE/ASME/ASEE Joint Propulsion Conference, AIAA-94-2980, Indianapolis, 1994.
24. Mell, E. R. (1991). Master's thesis, Cornell University.
25. Minck, R. W., *J. Appl. Phys*. 35:252 (1964).
26. Armstrong, R., Lucht, R., and Rawlins, W., *Appl. Optics* 22:1573 (1983).
27. DeMichelis, C., *IEEE J. Quantum Electronics* QE-5: 188 (1969).
28. Weyl, G. M., in *Laser-Induced Plasmas and Applications* (L. J. Radziemski and D. A. Cremers, Eds.), Marcel Dekker, New York, 1989, p. 1.
29. Root, R. G., in *Laser-Induced Plasmas and Applications* (L. J. Radziemski and D. A. Cremers, Eds.), Marcel Dekker, New York, 1989, p. 69.
30. Hauer, A. A., and Baldis, H. A., in *Laser-Induced Plasmas and Applications* (L. J. Radziemski and D. A. Cremers, Eds.), Marcel Dekker, New York, 1989, p. 105.
31. Lewis, B., and von Elbe, G., *Combustion, Flames and Explosions of Gases*, 3rd ed., Academic Press, New York, 1987, p. 215.
32. Sloane, T. M., *Combust. Sci. Technol*. 73:351 (1990).
33. Sloane, T. M., and Ronney, P. D., *Combust. Sci. Technol*. 88:1 (1992).
34. Taylor, G., *Proc. Roy. Soc*. A201:159 (1950).
35. Taylor, G., *Proc. Roy. Soc*. A201:175 (1950).
36. Klimkin, V. F., Soloukhin, R. I., and Wolansky, P., *Combust. Flame* 21:111 (1973).
37. Song, K. D., and Alexander, D. R., *J. Appl. Physics* 76:3297 (1994).
38. Song, K. D., and Alexander, D. R, *J. Appl. Physics* 76:3302 (1994).

Received 3 November 1998; revised 24 February 1999; accepted 7 April 1999